Received: 14 August 2019 | Revised: 28 April 2020 | Accepted: 1 May 2020

DOI: 10.1111/bph.15105

RESEARCH PAPER

Open-channel blocking action of volatile anaesthetics desflurane and sevoflurane on human voltage-gated $K_v1.5$ channel

Yutaka Fukushima[1,2] | Akiko Kojima[2] | Xinya Mi[1] | Wei-Guang Ding[1] | Hirotoshi Kitagawa[2] | Hiroshi Matsuura[1]

[1]Department of Physiology, Shiga University of Medical Science, Otsu, Japan

[2]Department of Anesthesiology, Shiga University of Medical Science, Otsu, Japan

Correspondence
Akiko Kojima, Department of Anesthesiology, Shiga University of Medical Science, Otsu, Shiga 520-2192, Japan.
Email: akiko77@belle.shiga-med.ac.jp

Funding information
JSPS (The Japan Society for the Promotion of Science, Tokyo, Japan) KAKENHI, Grant/Award Numbers: 17K08536, 17K11050, 18K16445

Background and Purpose: Volatile anaesthetics have been shown to differentially modulate mammalian *Shaker*-related voltage-gated potassium ($K_v1.x$) channels. This study was designed to investigate molecular and cellular mechanisms underlying the modulatory effects of desflurane or sevoflurane on human $K_v1.5$ ($hK_v1.5$) channels.

Experimental Approach: Thirteen single-point mutations were constructed within pore domain of $hK_v1.5$ channel using site-directed mutagenesis. The effects of desflurane or sevoflurane on heterologously expressed wild-type and mutant $hK_v1.5$ channels were examined by whole-cell patch-clamp technique. A computer simulation was conducted to predict the docking pose of desflurane or sevoflurane within $hK_v1.5$ channel.

Key Results: Both desflurane and sevoflurane increased $hK_v1.5$ current at mild depolarizations but decreased it at strong depolarizations, indicating that these anaesthetics produce both stimulatory and inhibitory actions on $hK_v1.5$ channels. The inhibitory effect of desflurane or sevoflurane on $hK_v1.5$ channels arose primarily from its open-channel blocking action. The inhibitory action of desflurane or sevoflurane on $hK_v1.5$ channels was significantly attenuated in T480A, V505A, and I508A mutant channels, compared with wild-type channel. Computational docking simulation predicted that desflurane or sevoflurane resides within the inner cavity of channel pore and has contact with Thr479, Thr480, Val505, and Ile508.

Conclusion and Implications: Desflurane and sevoflurane exert an open-channel blocking action on $hK_v1.5$ channels by functionally interacting with specific amino acids located within the channel pore. This study thus identifies a novel molecular basis mediating inhibitory modulation of $hK_v1.5$ channels by desflurane and sevoflurane.

1 | INTRODUCTION

Accumulating evidence has suggested that volatile anaesthetics have multiple protein targets, which prominently include ion channels, to produce anaesthetic and non-anaesthetic effects (Franks, 2006, 2008; Hemmings et al., 2005; Postea & Biel, 2011; Rudolph & Antkowiak, 2004). Volatile anaesthetics exert diverse effects on several classes of ion channels, including neurotransmitter-gated ion channels, two-pore-domain potassium channels, and voltage-gated ion channels. It is well known that anaesthetic potency, as evaluated by the minimum alveolar concentration (MAC), is greater in volatile

Abbreviations: Å, angstrom; hERG, human ether-a-go-go-related gene; MAC, minimum alveolar concentration; TM, transmembrane; WT, wild type.

anaesthetics **desflurane** and **sevoflurane** than in the conventional gas anaesthetic, nitrous oxide (1 MAC: desflurane, 6%; sevoflurane, 2%; nitrous oxide, 105%; Aranake, Mashour, & Avidan, 2013). Previous studies, using voltage-clamp electrophysiology, site-directed mutagenesis, photoaffinity labelling, and computational docking simulations, have detected the putative binding sites for volatile anaesthetics in ion channels (Liu, Willenbring, Xu, & Tang, 2009; Mihic et al., 1997; Nishikawa & Harrison, 2003; Siegwart, Krähenbühl, Lambert, & Rudolph, 2003; Woll et al., 2018), which appear to be involved in mediating a direct functional modulation of various types of cells, including neuronal, cardiac, and smooth muscle cells (Hudson, Herold, & Hemmings, 2018).

The voltage-gated potassium channel family, which comprises the most diverse subgroups among voltage-gated ion channel superfamily, plays key roles in controlling membrane potential and thereby cellular excitability in various cell types (Yellen, 2002). Accordingly, a number of studies have examined the regulatory effect of volatile anaesthetics on various voltage-gated potassium channels to elucidate ionic mechanisms underlying modulation of cellular functions by volatile anaesthetics (Friederich, Benzenberg, Trellakis, & Urban, 2001; Kang et al., 2006; Kojima, Ito, Kitagawa, Matsuura, & Nosaka, 2014). The *Shaker*-related voltage-gated potassium (K_v1.x) channel family contributes to many cellular processes, such as regulation of neurotransmitter release (Trimmer, 2015), vascular tone (Cogolludo et al., 2006; Hayabuchi, 2017), and cardiac atrial refractoriness (Wettwer et al., 2004), and represents a target for the action of volatile anaesthetics (Covarrubias, Barber, Carnevale, Treptow, & Eckenhoff, 2015; Li et al., 2018; Lioudyno et al., 2013). For example, a previous voltage-clamp experiment using the *Xenopus* oocyte heterologous expression system demonstrated that sevoflurane potentiates mammalian **K_v1.2** channels by increasing the maximal conductance and causing a hyperpolarizing shift of conductance–voltage relationships (Barber, Liang, & Covarrubias, 2012). A subsequent study using azisevoflurane, a photoaffinity ligand for sevoflurane, suggested that Leu317, located within internal S4-S5 linker of K_v1.2 channels, is a sevoflurane binding site, associated with its positive modulatory effect (Woll et al., 2017). Because the internal S4-S5 linker contributes to voltage-dependent activation gating of K_v1.2 channels (Covarrubias et al., 2015; Harris, Graber, & Covarrubias, 2003), it seems likely that sevoflurane interacts with the channel gate region, including S4-S5 linker, to produce positive modulation on mammalian *Shaker*-related voltage-gated potassium channels.

On the other hand, previous studies using mammalian cell lines have found that sevoflurane exerts stimulatory and inhibitory effects on human **K_v1.5** (hK_v1.5) channels in a voltage-dependent manner (Li et al., 2018; Lioudyno et al., 2013). However, the molecular and cellular mechanisms underlying the inhibitory effect of volatile anaesthetics on hK_v1.5 channels have yet to be fully elucidated. The present study used site-directed mutagenesis combined with patch-clamp technique as well as computational docking simulation to investigate the modulatory effects of desflurane and sevoflurane on hK_v1.5 channels. We found that both desflurane and sevoflurane exert an open-channel blocking action on hK_v1.5 channels through functional interaction with specific amino acids located within the channel pore.

What is already known

- Volatile anaesthetics differentially modulate mammalian *Shaker*-related voltage-gated potassium (Kv1) channels regulating neuronal and cardiovascular functions.

What this study adds

- Desflurane and sevoflurane block hK_v1.5 channels in an open-state by interacting with specific amino acids.

What is the clinical significance

- Volatile anaesthetics directly interact with hK_v1.5 channels and thereby modulate cardiovascular function in clinical settings.

2 | METHODS

2.1 | Cell culture, site-directed mutagenesis, and transfection

CHO (RRID:CVCL_0213) cells were maintained at 37°C in DMEM/Ham's F-12 medium supplemented with 10% FBS and antibiotics (100 units ml^{-1} penicillin and 100 μg ml^{-1} streptomycin) in a humidified atmosphere with 95% air and 5% CO_2. The cells were passaged twice a week, and a fraction of cells was plated onto glass coverslips (3×5 mm^2) in 35-mm culture dishes, 24 h before transfection. The mammalian expression vector pcDNA3.1 containing full-length cDNA encoding the wild-type (WT) hK_v1.5 channel (human KCNA5; GenBank accession number NM_002234) was kindly provided by Professor David Fedida (University of British Columbia, Canada). The hK_v1.5 channel underlies the ultra-rapidly activating delayed rectifier K^+ current in the heart (I_{Kur}) and comprises 613 amino acids within its pore-forming α-subunit, which is composed of six transmembrane spanning segments (S1 to S6; Fedida et al., 1993). Previous mutagenesis studies have shown that amino acids located within the pore domain of hK_v1.5 channels are primarily involved in mediating the action of its open-channel blockers, such as S0100176, AVE0118, vernakalant and **propofol** (Decher et al., 2004; Decher, Kumar, Gonzalez, Pirard, & Sanguinetti, 2006; Eldstrom et al., 2007; Eldstrom & Fedida, 2009; Kojima et al., 2018; Kojima, Ito, Ding, Kitagawa, & Matsuura, 2015). In the present study, we therefore mutated the following 13 amino acids in the pore domain; Thr462 and

His463 (located at pore turret), Thr479 and Thr480 (located at the base of the ion selectivity filter), Arg487 (located at the external entryway of the pore), and Ala501, Ile502, Val505, Ile508, Ala509, Leu510, Val512, and Val516 (located within the S6 segment) within the $hK_v1.5$ channel α-subunit, using PCR-based site-directed mutagenesis with a QuikChange Kit (Stratagene, La Jolla, CA, USA). These are T462C, H463C, T479A, T480A, R487V, A501V, I502A, V505A, I508A, A509G, L510A, V512A, and V516A mutants of $hK_v1.5$ channel. The full-length cDNA encoding the human WT KCNQ1 (hKCNQ1 or $hK_v7.1$; GenBank accession number AF000571, a kind gift from Professor Jacques Barhanin, Institut de Pharmacologie Moléculaire et Cellulaire, CNRS, Valbonne, France) was subcloned into a pIRES2-eGFP expression vector (Nishio et al., 2009). The full-length cDNA encoding human WT KCNE1 (hKCNE1; GenBank accession number M26685) subcloned into pcDNA3.1 was constructed using PCR from the human heart cDNA library (Clontech Laboratories, Mountain View, CA, USA). It is established that hKCNQ1 and hKCNE1 genes, respectively, encode pore-forming α-subunits and ancillary β-subunits of slowly activating delayed rectifier K^+ channel in human heart (I_{Ks}; Keating & Sanguinetti, 2001). The full-length cDNA encoding WT human ether-a-go-go-related gene (hERG or $hK_v11.1$; GenBank accession number AF363636, a kind gift from Professor Michael Sanguinetti, University of Utah, Salt Lake City, UT, USA) channel was subcloned into pRc/CMV expression vector. The hERG encodes pore-forming α-subunits of the rapidly activating delayed rectifier K^+ channel in human heart (I_{Kr}; Keating & Sanguinetti, 2001). The sequence of each construct was verified using ABI PPISM 3130xl sequencer (Applied Biosystems, Foster City, CA, USA) before the expression study. The cDNAs for WT or mutant $hK_v1.5$ channels and WT hERG channels (0.5–1 μg) were transiently transfected into CHO cells together with GFP cDNA (0.5 μg) using Lipofectamine (Invitrogen Life Technologies, Carlsbad, CA, USA). hKCNQ1 (0.5 μg) and hKCNE1 cDNAs (0.5 μg) were cotransfected into CHO cells using Lipofectamine. Electrophysiological experiments were conducted on GFP-positive cells approximately 48 h after transfection.

2.2 | Whole-cell patch-clamp recordings and data analysis

Patch-clamp technique (Hamill, Marty, Neher, Sakmann, & Sigworth, 1981) was applied to CHO cells in whole-cell mode using an EPC-8 amplifier (HEKA Elektronik, Lambrecht, Germany). Data were usually low-pass filtered at 1 kHz and sampled at 5 kHz through an ITC-16 analogue-to-digital converter (Instrutech, NY, USA). The data were stored on a computer using PULSE/PULSEFIT software program (HEKA Elektronik). Series resistance compensation was employed up to 80% to minimize voltage errors.

The bath solution for recording $hK_v1.5$, hERG, and hKCNQ1/hKCNE1 currents was normal Tyrode solution containing (in mM) 140 NaCl, 5.4 KCl, 1.8 $CaCl_2$, 0.5 $MgCl_2$, 0.33 NaH_2PO_4, 5.5 glucose, and 5.0 HEPES (pH adjusted to 7.4 with NaOH). Pipette solution for recording $hK_v1.5$, hERG, and hKCNQ1/hKCNE1 currents contained (in mM) 70 potassium aspartate, 40 KCl, 10 KH_2PO_4, 1 $MgSO_4$, 3 ATP (disodium salt; Sigma Chemical Company, St Louis, MO, USA), 0.1 GTP (dilithium salt; Sigma), 5 EGTA, and 5 HEPES (pH adjusted to 7.2 with KOH). Patch electrode was fabricated from glass capillaries (outer diameter, 1.5 mm; inner diameter, 0.9 mm; Narishige Scientific Instrument Laboratory, Tokyo, Japan) using a horizontal microelectrode puller (P-97; Sutter Instrument, Novato, CA, USA), and the tip was then fire-polished using an MF-830 microforge (Narishige Scientific Instrument Laboratory). The electrodes had a resistance of 2.5 to 4.0 MΩ when filled with pipette solution. A glass coverslip with adherent CHO cells was transferred to a recording chamber (0.5 ml in volume) mounted on the stage of an inverted microscope (ECLIPSE TE2000-U, Nikon, Tokyo, Japan), and was continuously superfused with normal Tyrode solution (36–37°C) at the rate of 2 ml min^{-1}.

The $hK_v1.5$ current was activated by 300-ms depolarizing voltage-clamp steps applied from a holding potential of −80 mV to test potentials of −50 to +50 mV in 10-mV steps (every 6 s), followed by repolarization to −40 mV to elicit the tail current. The amplitude of $hK_v1.5$ current was measured at the start and end of 300-ms depolarizing steps (initial and late current levels, respectively). The concentration–response relationships for the inhibition of $hK_v1.5$ current by anaesthetics were constructed by measuring the reduction in the late current amplitude caused by anaesthetics relative to the control at a test potential of +30 mV (percent inhibition). This percent inhibition was fitted with a Hill equation as follows:

$$\text{percent inhibition} = 1/\left(1 + \left(IC_{50}/[\text{anaesthetic}]\right)^{n_H}\right),$$

where IC_{50} is the concentration of anaesthetic causing a half-maximal inhibition, [anaesthetic] is the concentration of desflurane or sevoflurane, and n_H is the Hill coefficient. In the Hill fitting, the concentrations of anaesthetics were presented in the millimolar order. The time course of $hK_v1.5$ current decline during depolarizing step to +30 mV in the absence ($I_{Control}$) and presence of desflurane ($I_{Desflurane}$) or sevoflurane ($I_{Sevoflurane}$) was evaluated by fitting with a single exponential function to obtain time constant (τ). The anaesthetic-induced inhibition of $hK_v1.5$ current during a 300-ms depolarizing step was evaluated by fitting a single exponential function to the current ratio ($I_{Desflurane}/I_{Control}$ or $I_{Sevolurane}/I_{Control}$), obtained by dividing the $hK_v1.5$ current in the presence of anaesthetic by that in its absence at test potentials of ≥−10 mV. The effects of anaesthetics on deactivation kinetics of $hK_v1.5$ channels were assessed by fitting a single exponential function to the tail currents elicited upon repolarization to −40 mV after a depolarizing step to the test potential of +30 mV in the absence or presence of anaesthetics. The horizontal line to the left of current traces indicates the zero-current level.

The hERG and hKCNQ1/hKCNE1 currents were activated by 2-s depolarizing steps to test potentials of −50 to +50 mV applied from a holding potential of −80 mV, followed by repolarization to −50 mV to elicit tail current. We also measured the amplitudes of tail currents for $hK_v1.5$, hERG, and hKCNQ1/hKCNE1 channels, which reflect the degree of channel activation at the preceding depolarizing test potentials. The effect of desflurane or sevoflurane on the

voltage-dependent activation of hKv1.5, hERG, or hKCNQ1/hKCNE1 current was evaluated by the current–voltage relationship for the tail current fitted with a Boltzmann equation:

$$I_{tail} = I_{tail,max}/(1 + \exp((V_h - V_m)/k)),$$

where $I_{tail,max}$ is the fitted maximal tail current density, I_{tail} is tail current amplitude at each test potential normalized to its amplitude at +50 mV in control, V_h is the voltage at half-maximal activation, V_m is the test potential, and k is the slope factor. The inhibitory action of desflurane on hERG or hKCNQ1/hKCNE1 current was evaluated by measuring the reduction in the tail current amplitude caused by desflurane relative to the control at a test potential of +30 mV (percent inhibition). The concentration–response relationship was constructed from the percent inhibition caused by each concentration of desflurane and fitted with a Hill equation to yield IC_{50}.

2.3 | Docking simulation study

The $hK_v1.5$ channel modelling, desflurane or sevoflurane docking, and three-dimensional representation were conducted using the Molecular Operating Environment (MOE, version 2016.0802; Chemical Computing Group, Inc., Quebec, Canada). A homology model of $hK_v1.5$ channels was constructed based on the 2.9 Å crystal structure of rat $K_v1.2$ channel (Protein Data Bank code: 2A79; Long, Campbell, & Mackinnon, 2005), which is believed to represent the open-state of the channel. This $hK_v1.5$ homology model comprised amino acid residues from Asp207 to Thr527 and included S1-S6 domain. The hydrogens were added to $hK_v1.5$ channel protein and then optimized using Protonate 3D program (Corbeil, Williams, & Labute, 2012; Labute, 2009). $hK_v1.5$ channel structure was optimized by energy minimization. Desflurane or sevoflurane was docked to the $hK_v1.5$ model, using ASEDock (2016.0107; Bai, Ding, Kojima, Seto, & Matsuura, 2015; Goto, Kataoka, Muta, & Hirayama, 2008). We adopted the AMBER10:EHT force field to set partial charge and force-field parameters, and used the generalized born/volume integral (GB/VI) implicit solvent model (Labute, 2008) to estimate solvation energies. During the docking simulation, the structures of side chain atoms within the $hK_v1.5$ channel were kept flexible, while the movement of main chain atoms was restrained with a harmonic potential of 100 kcal mol^{-1} $Å^{-2}$ (Chutiwitoonchai et al., 2011). The structure of the ligand was kept flexible during the docking simulation. To evaluate possible docking sites, the number of docking solutions per site was counted in top 100 poses of desflurane or sevoflurane docked to the hKv1.5 homology model, determined by docking scores composed of electrostatic, van der Waals, solvation, and strain energy (Goto et al., 2008; Mori et al., 2012). The $hK_v1.5$ channel protein was divided into seven possible regions, namely, inner cavity of the channel pore, S6-pore helix interface, extracellular face, S4-S5 linker, voltage-sensor domain, S4-pore interface (Stock, Hosoume, Cirqueira, & Treptow, 2018; Stock, Hosoume, & Treptow, 2017), and other locations.

Furthermore, we calculated the docking pose of desflurane or sevoflurane by predicting its active-site within the inner cavity of the channel pore using a Site Finder (Chutiwitoonchai et al., 2011; Hiasa et al., 2013). The amino acids with side chain atoms located within 4.5 Å of the docked anaesthetics were regarded as having a potential contact. To evaluate the contribution of individual amino acids within $hK_v1.5$ channels towards anaesthetic interaction, we conducted in silico alanine scanning mutagenesis using Residue Scan module of MOE (Liu, Peng, Zhou, Zhang, & Zhang, 2018; Saponara et al., 2016), where a specific amino acid, predicted to have potential contact with anaesthetics, was mutated to alanine. The binding free energy (ΔG) was calculated before and after the mutation using GBVI/WSA dG (Generalized-Born Volume Integral/Weighted Surface area) scoring function (Corbeil et al., 2012), and the difference in binding free energies ($\Delta\Delta G$) was determined as follows:

$$\Delta\Delta G = \Delta G_{mutant} - \Delta G_{WT},$$

where ΔG_{mutant} is the binding free energy for anaesthetic to the mutated $hK_v1.5$ channel and ΔG_{WT} is the binding free energy for anaesthetic to WT $hK_v1.5$ channel.

2.4 | Data and statistical analysis

The data and statistical analysis comply with the recommendations of the *British Journal of Pharmacology* on experimental design and analysis in pharmacology (Curtis et al., 2018). Data are presented as the mean ± SD, and the number of cells obtained from independent experiments is indicated by *n*. The statistical power analysis predicted that a group size of $n = 6$ would allow detection of a difference of 25% between group means in the percent inhibition of WT and mutant $hK_v1.5$ channels by desflurane, assuming a statistical power of 0.95 at a significance level (α) of 0.05 using StatMate Version 2.0b (RRID:SCR_000306; GraphPad Software, La Jolla, CA, USA).

WT and 13 mutant $hK_v1.5$ channel cDNAs were randomly selected and transfected into CHO cells. Data recording and the analysis were not performed in a blinded manner because the current traces of WT and mutant $hK_v1.5$ channels could be readily distinguished based on their electrophysiological properties. Unless otherwise stated, we evaluated the effects of desflurane or sevoflurane on WT or mutant $hK_v1.5$ channels by comparing the late current amplitudes measured at +30 mV in the absence and presence of anaesthetics in the same cells, which avoided the differences in current amplitude among cells that may arise from the differences in $hK_v1.5$ channel expression levels. Alternatively, we normalized the initial and late current amplitude of WT $hK_v1.5$ channels at each test potential in the absence and presence of anaesthetics with reference to the initial current amplitude at +50 mV in the absence of anaesthetics, which also compensated for the differences in current amplitude among cells.

Statistical comparisons were performed using Student's two-tailed *t* test or an ANOVA with GraphPad Prism (RRID:SCR_002798;

GraphPad Software), as appropriate. When *F* achieved the level of statistical significance after ANOVA, Dunnett's post hoc test was run. *P* values of <0.05 were considered to indicate statistical significance.

2.5 | Materials

Desflurane (2-(difluoromethoxy)-1,1,1,2-tetrafluoroethane; Baxter, Deerfield, IL, USA) or sevoflurane (1,1,1,3,3,3-hexafluoro-2-(fluoromethoxy)propane; Abbott Laboratories, North Chicago, IL, USA) was equilibrated in normal Tyrode solution in a reservoir by passing air (flow rate, 0.5 L min^{-1}) through an anaesthetic vaporizer (desflurane, Tec 6 Plus; GE Healthcare Japan, Tokyo, Japan; sevoflurane, Tec 7; GE Healthcare Japan, Tokyo, Japan). Gas chromatography was used to measure the concentration of desflurane or sevoflurane in the normal Tyrode solution superfusing the cells within the recording chamber at 36–37°C (GC-14B; Shimadzu, Kyoto, Japan), and the results were as follows: 0.49 ± 0.05 (*n* = 4), 0.95 ± 0.09 (*n* = 4), and 1.55 ± 0.23 mM (*n* = 4) for 6%, 12%, and 18% desflurane and 0.27 ± 0.01 (*n* = 4), 0.59 ± 0.01 (*n* = 4), 0.90 ± 0.02 mM (*n* = 4), and 1.35 ± 0.03 mM (*n* = 4) for 2%, 4%, 6%, and 8% sevoflurane, respectively.

2.6 | Nomenclature of targets and ligands

Key protein targets and ligands in this article are hyperlinked to corresponding entries in http://www.guidetopharmacology.org,

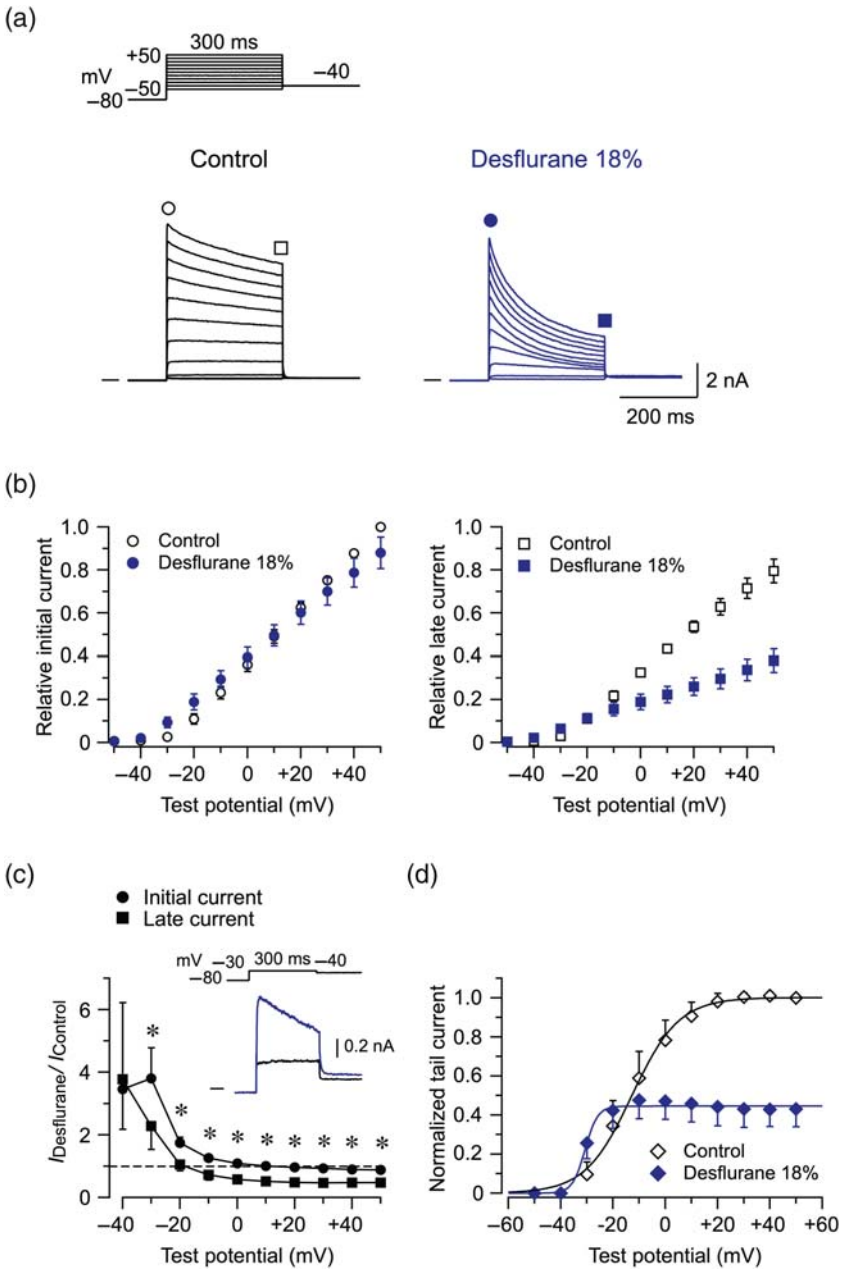

FIGURE 1 Effect of desflurane on $hK_v1.5$ channels heterologously expressed in CHO cells. (a) Superimposed traces of $hK_v1.5$ currents activated during 300-ms depolarizing voltage-clamp steps to test potentials of −50 to +50 mV in 10-mV steps applied from a holding potential of −80 mV, before (left panel) and 7 min after exposure to 18% desflurane (right panel). Voltage-clamp protocol is illustrated above the control traces of $hK_v1.5$ current. (b) Current–voltage relationships for the initial (left panel) and late current levels (right panel) measured during depolarizing steps in the absence (Control) and presence of 18% desflurane. Amplitude of initial or late current at each test potential was normalized with reference to its initial current amplitude measured at +50 mV in control (*n* = 6). (c) Current ratio of initial and late currents, obtained by dividing the current amplitude in the presence of desflurane by that in its absence at each test potential, in the experimental results shown in panel (b). The dashed line indicates $I_{Desflurane}/I_{Control}$ = 1. Note that while the initial current ratio was more than 1 at potentials between −40 and 0 mV, the late current ratio was more than 1 at potentials between −40 and −20 mV. *P < 0.05 between the initial and late current ratios. (d) The current–voltage relationships for the tail currents of $hK_v1.5$ channels measured upon repolarization to −40 mV from various test potentials in the absence and presence of 18% desflurane. The smooth curves through the data points represent least-squares fittings of the Boltzmann equation to the data points, yielding V_h (V_h, −12.5 ± 5.0 mV in control; −30.0 ± 1.2 mV in the presence of 18% desflurane, *n* = 6)

the common portal for data from the IUPHAR/BPS Guide to PHARMACOLOGY (Harding et al., 2018), and are permanently archived in the Concise Guide to PHARMACOLOGY 2019/20 (Alexander et al., 2019).

3 | RESULTS

3.1 | Modulatory effects of desflurane on $hK_v1.5$ current

Figure 1a shows the effect of 18% desflurane on $hK_v1.5$ current, activated by depolarizing steps to various test potentials between −50 and +50 mV. The $hK_v1.5$ current was appreciably activated at potentials of ≥−30 mV and exhibited a modest decline during strong depolarizations, due to slow P/C type inactivation (Eduljee, Claydon, Viswanathan, Fedida, & Kehl, 2007). Figure 1b illustrates the normalized current–voltage relationships for the initial (left panel) and late current levels (right panel) of $hK_v1.5$ current in the absence and presence of 18% desflurane. To quantitatively evaluate the modulatory effect of desflurane on hKv1.5 current, we measured the current ratio in the presence and absence of desflurane ($I_{Desflurane}/I_{Control}$) for the initial and late current levels at each test potential (Figure 1c). Both the initial and late current ratios were >1 at less depolarized potentials but decreased to <1 with strong depolarizations, showing that 18% desflurane had both stimulatory and inhibitory effects on $hK_v1.5$ current, depending on the degree of membrane depolarization. Desflurane (18%) shifted the voltage dependence of $hK_v1.5$ current activation to a hyperpolarizing direction, as evaluated by current–voltage relationships for the tail currents (Figure 1d), which appears to arise from the stimulatory action of desflurane at mild depolarizations as well as inhibitory action at strong depolarizations.

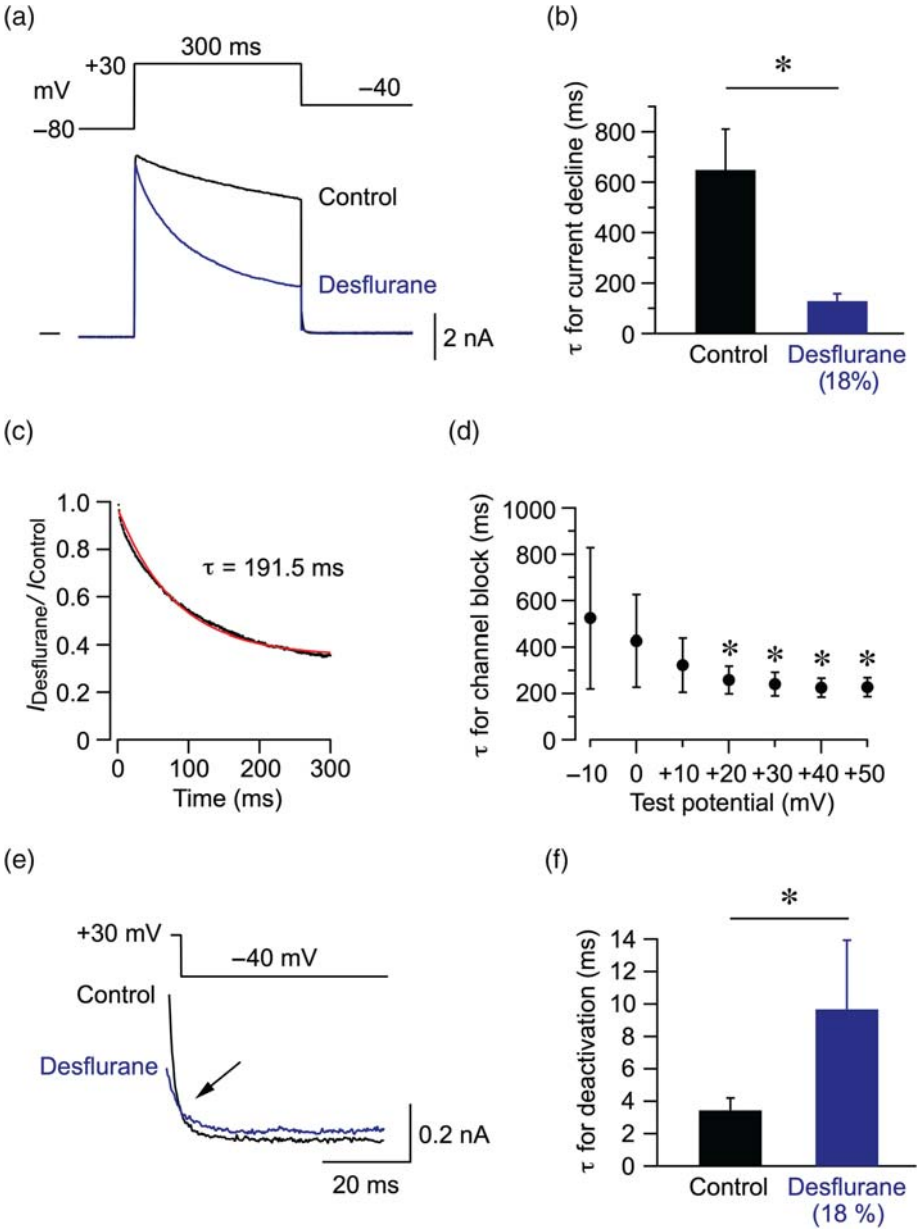

FIGURE 2 Open-channel blocking effect of desflurane on $hK_v1.5$ channels. (a) Superimposed $hK_v1.5$ currents recorded during 300-ms depolarizing steps to +30 mV before and during exposure to 18% desflurane. (b) Time constant (τ) for the $hK_v1.5$ current decline during 300-ms depolarizing steps in the absence (Control) and presence of 18% desflurane, obtained by least-squares fitting of the single exponential function. *$P < 0.05$ between control and 18% desflurane groups ($n = 6$). (c) The current ratio ($I_{Desflurane}/I_{Control}$) obtained by dividing $hK_v1.5$ current in the presence of 18% desflurane ($I_{Desflurane}$) by that in its absence ($I_{Control}$), shown in Figure 2a. The smooth curve through the data points (red) represents a least-squares fit of a single exponential function, yielding a time constant for channel block (τ). (d) Time constant (τ) for $hK_v1.5$ channel inhibition by desflurane at various test potentials ($n = 6$). *$P < 0.05$, compared with τ at −10 mV. (e) Superimposed tail currents elicited upon repolarization to −40 mV following depolarizing steps to +30 mV in the absence (Control) and presence of 18% desflurane. The arrow shows crossover of tail currents. (f) Time constant (τ) for the decay of tail currents in the absence (Control) and presence of 18% desflurane, obtained by a least-squares fit of the single exponential function. *$P < 0.05$ between control and 18% desflurane groups ($n = 6$)

3.2 | Open-channel block of $hK_v1.5$ current by desflurane

Figure 2a shows superimposed traces of $hK_v1.5$ current recorded during 300-ms depolarizing voltage step to +30 mV before and during exposure to 18% desflurane. The time course of the $hK_v1.5$ current decline during depolarizing steps, as evaluated by least-squares fitting to single exponential function, was much faster in the presence of desflurane than in control (Figure 2b). To evaluate the time course of the desflurane-induced acceleration of $hK_v1.5$ current decline during depolarizing steps, we calculated and analysed the current ratio in the presence and absence of desflurane ($I_{Desflurane}/I_{Control}$), which represents the fraction of $hK_v1.5$ current that is not inhibited by 18% desflurane (Figure 2c). This current ratio was approximately 1 at the onset of depolarization but then gradually decreased to approximately 0.4 at the end of 300-ms depolarizing step, showing that desflurane-induced inhibition of $hK_v1.5$ current was not apparent at the onset of depolarization but gradually proceeded during 300 ms of depolarization. The time course of desflurane-induced inhibition of $hK_v1.5$ current during depolarization was also quantitatively analysed by fitting a single exponential function to the current ratio ($I_{Desflurane}/I_{Control}$). The time constant ($\tau$) for $hK_v1.5$ current decline was significantly smaller at test potentials of +20 to +50 mV than at −10 mV (Figure 2d), suggesting that the desflurane-induced inhibition of $hK_v1.5$ channels was accelerated at more depolarized potentials, where the open probability of $hK_v1.5$ channels became elevated (see also Figure 1d).

The tail current elicited upon repolarization reflects the deactivation process of the channel from the open-state to closed-state.

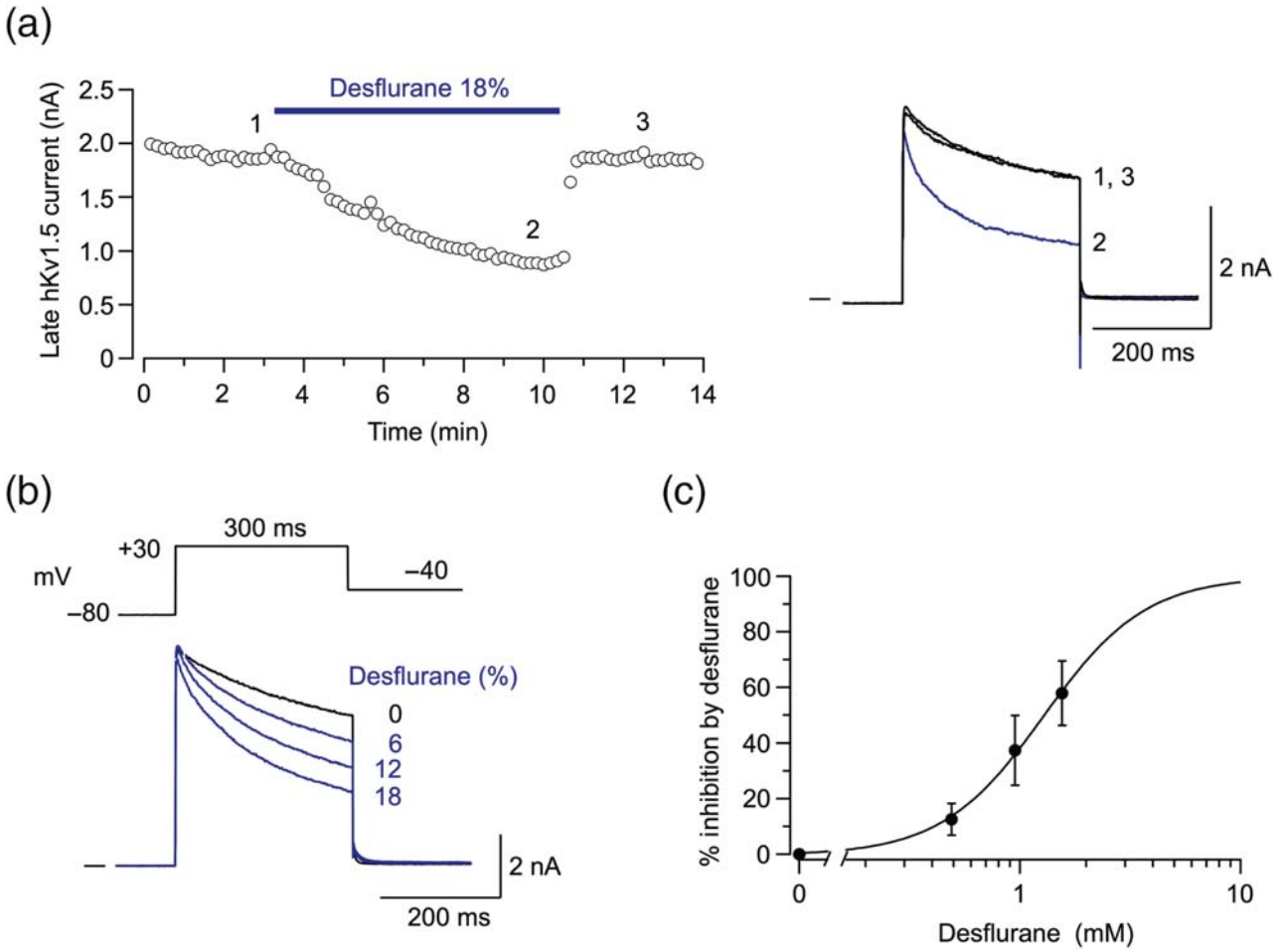

FIGURE 3 Reversibility and concentration dependence of desflurane-induced inhibition of $hK_v1.5$ current. (a) Changes in the late current amplitude of $hK_v1.5$ current, activated by 300-ms depolarizing step to +30 mV every 10 s, before, during exposure to 18% desflurane, and after its washout. The desflurane-induced reduction of $hK_v1.5$ current reached a maximum approximately 7 min after the application of desflurane, and then it was completely recovered to the control level after the washout of 18% desflurane. The horizontal bar indicates the period of desflurane application. The inset (right panel) shows the original current traces obtained at the time points indicated by numerals. (b) Superimposed traces of $hK_v1.5$ current recorded during 300-ms depolarizing step to +30 mV before and during exposure to increasing concentrations of desflurane (6%, 12%, and 18%) applied in a cumulative manner. A higher concentration of desflurane was applied after the response to the previous concentration reached a steady state (usually 3 min). (c) Mean concentration–response relationships for the inhibition of $hK_v1.5$ current by desflurane. The data points (n = 6) represent the percent inhibition of late current, calculated as the reduction with respect to control measured at the end of 300-ms depolarizing step to +30 mV and fitted with the Hill equation. The concentration of desflurane is shown in the millimolar order

Desflurane not only decreased the amplitude of tail current but also decelerated its decaying time course (Figure 2e). These two phenomena combined to produce a crossover of tail currents recorded in the absence and presence of desflurane. In fact, 18% desflurane significantly increased the deactivation time constant (τ, Figure 2f), confirming that channel deactivation was decelerated by desflurane. It is generally accepted that the normal deactivation of the channel is prevented by the compound (open-channel blocker) that enters and binds to the inner cavity of channel pore during its open-state (Decher et al., 2006; Eldstrom et al., 2007). Both the time-dependent development of channel inhibition during depolarization (Figure 2c) and the slowing of channel deactivation (Figure 2f) suggest that desflurane preferentially affects the $hK_v1.5$ channels in an open-state.

3.3 | Reversible and concentration-dependent block of $hK_v1.5$ current by desflurane

As demonstrated in Figure 3a, desflurane-induced inhibition of $hK_v1.5$ current was completely reversible after its removal. Figure 3b demonstrates superimposed traces of $hK_v1.5$ current recorded at a test potential of +30 mV before and during exposure to increasing concentrations of desflurane (6%, 12%, and 18%) applied in a cumulative manner. Desflurane blocked the $hK_v1.5$ current in a concentration-dependent manner with an IC_{50} of 1.36 ± 0.28 mM (which corresponds to 16.2 ± 3.5%; Figure 3c).

3.4 | Mutational analysis of desflurane-induced block of $hK_v1.5$ channel

We then examined the inhibitory effects of desflurane on various mutant $hK_v1.5$ channels to predict the sites for desflurane interaction with $hK_v1.5$ channel. As demonstrated in Figure 4, the degree of $hK_v1.5$ current inhibition by 18% desflurane, measured at +30 mV, was not affected in T462C, H463C, T479A, R487V, A501V, L510A, and V512A mutant channels. However, inhibitory effect of desflurane was significantly attenuated in T480A, V505A, and I508A and was potentiated in A509G mutant, compared with WT channel. In contrast, interestingly, 18% desflurane increased current amplitudes in I502A and V516A mutant channels.

Because the degree of $hK_v1.5$ current inhibition by desflurane was significantly altered in T480A, V505A, I508A, and A509G mutant channels (Figure 4b), we further characterized the inhibitory potency of desflurane on these mutant channels to compare with WT channel. Figure 5a shows superimposed current traces recorded from four

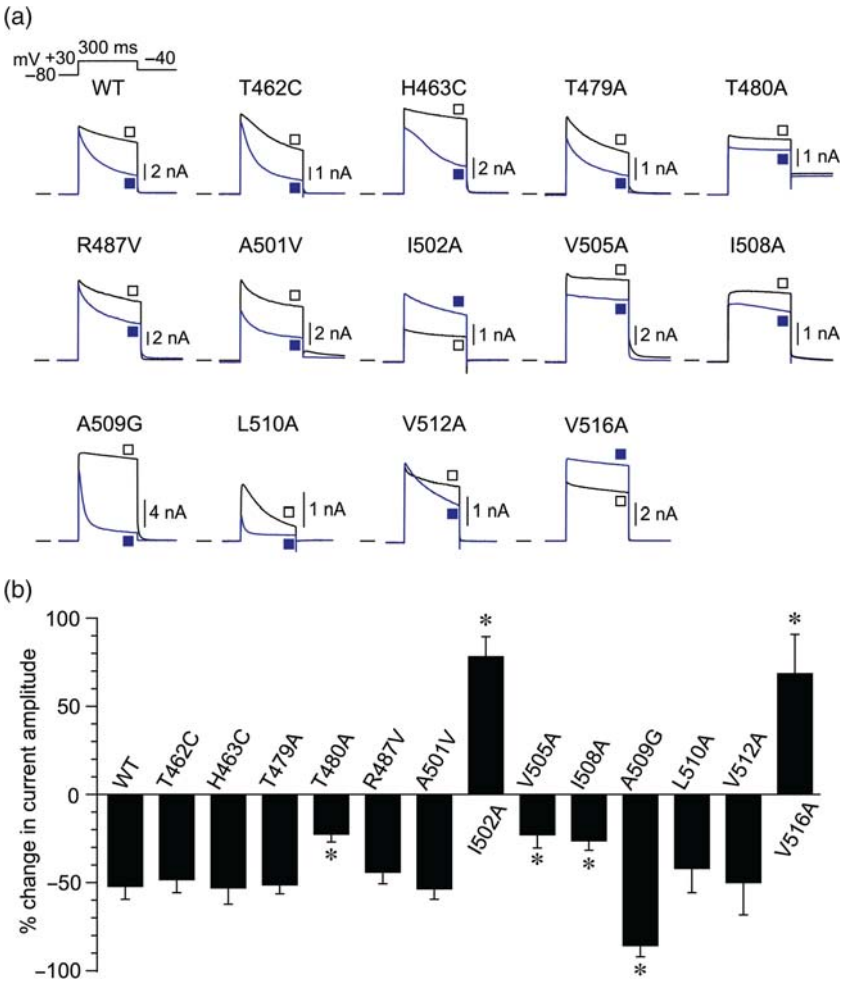

FIGURE 4 Effect of 18% desflurane on wild-type (WT) and mutant $hK_v1.5$ channel currents. (a) Superimposed current traces recorded from WT and 13 mutant $hK_v1.5$ channels (T462C, H463C, T479A, T480A, R487V, A501V, I502A, V505A, I508A, A509G, L510A, V512A, and V516A) during 300-ms depolarizing steps to +30 mV in the absence (open square) and presence (filled square) of 18% desflurane. (b) Percent change in the late current amplitude at +30 mV caused by 18% desflurane in WT and 13 mutant $hK_v1.5$ channel currents. *$P < 0.05$, compared with WT. $n = 6$ in each group

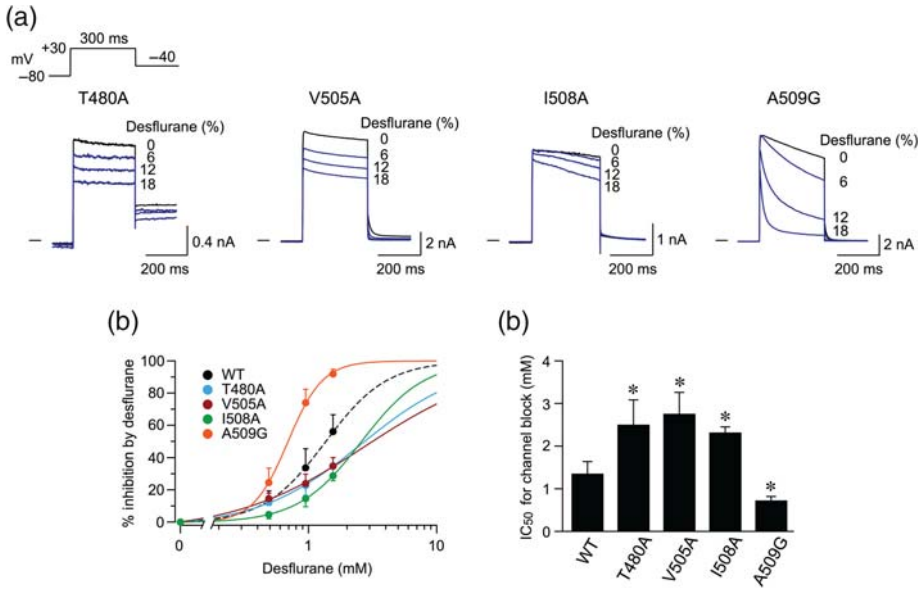

FIGURE 5 The concentration dependence of desflurane-induced inhibition in mutant $hK_v1.5$ channels. (a) Superimposed current traces recorded from mutant (T480A, V505A, I508A, and A509G) $hK_v1.5$ channels during 300-ms depolarizing step to +30 mV in the absence and presence of 6%, 12%, and 18% desflurane applied in a cumulative way. (b) The mean concentration–response relationships for the inhibition of late current at +30 mV in wild-type (WT) and four mutant (T480A, V505A, I508A, and A509G) $hK_v1.5$ channels. The dashed curve (WT) and continuous curves (T480A, V505A, I508A, and A509G) through data points represent a least-squares fit of Hill equation, yielding IC_{50} values. (c) IC_{50} values for WT and mutant (T480A, V505A, I508A, and A509G) hKv1.5 channels. The desflurane concentration is expressed as millimolar order in panels (b) and (c). *$P < 0.05$, compared with WT. $n = 6$ in each group

mutant (T480A, V505A, I508A, and A509G) $hK_v1.5$ channels, before and during exposure to increasing concentrations (6%, 12%, and 18%) of desflurane. The IC_{50} value for the desflurane-induced inhibition of $hK_v1.5$ channels was significantly increased in T480A, V505A, and I508A but was decreased in A509G mutant channel (Figure 5b,c), indicating that the inhibitory potency of desflurane was significantly attenuated in T480A, V505A, and I508A but was potentiated in A509G mutant $hK_v1.5$ channels. These results strongly suggest that Thr480, Val505, Ile508, and Ala509 act as key amino acids to determine the sensitivity of $hK_v1.5$ channels to inhibition by desflurane.

3.5 | Open-channel block of $hK_v1.5$ current by sevoflurane

We next examined the modulatory effect of sevoflurane on $hK_v1.5$ current. As shown in Figure 6a–c, sevoflurane produced both stimulatory and inhibitory effects on $hK_v1.5$ current in a voltage-dependent manner, in a way similar to that of desflurane (Figure 1). The voltage dependence of $hK_v1.5$ current activation was also shifted to a negative direction by sevoflurane (Figure 6d,e). Sevoflurane decreased late $hK_v1.5$ current, measured at +30 mV, in a concentration-dependent manner with an IC_{50} of 1.01 ± 0.14 mM (Figure 6f), which corresponds to 6.9 ± 1.0%.

Sevoflurane (8%) markedly accelerated the decline in $hK_v1.5$ current during 300-ms depolarizing steps to +30 mV (Figure 7a), as shown by a significant reduction in τ for current decline (Figure 7b). The current ratio ($I_{Sevoflurane}/I_{Control}$), which indicates the fraction of $hK_v1.5$ current that is not inhibited by 8% sevoflurane, was approximately 1 at the onset of depolarization but then gradually decreased to approximately 0.4 at the end of 300-ms depolarizing step, with a time constant (τ) of 129.1 ms (Figure 7c). The time constant (τ) for $hK_v1.5$ channel block was significantly smaller at test potentials of +10 to +50 mV than at −10 mV (Figure 7d), suggesting that the sevoflurane-induced inhibition of $hK_v1.5$ channels was facilitated at more depolarized potentials. The crossover of tail currents was also observed in the absence and presence of sevoflurane (Figure 7e), which could be ascribed to decelerated deactivation by sevoflurane (Figure 7f). These observations are consistent with sevoflurane acting as an open-channel blocker on $hK_v1.5$ channels, similar to the action of desflurane.

3.6 | Mutational analysis of sevoflurane-induced block of $hK_v1.5$ channel

The inhibitory effect of 8% sevoflurane was significantly attenuated in T480A, V505A, and I508A but was potentiated in A509G mutant channels, compared with WT $hK_v1.5$ channel (Figure 8). Sevoflurane inhibited the remaining mutant channels to a degree similar to the WT channel. In contrast, sevoflurane increased the current amplitude in I502A and V516A mutant $hK_v1.5$ channels. These mutagenesis results of sevoflurane were qualitatively similar to those of desflurane (Figure 4).

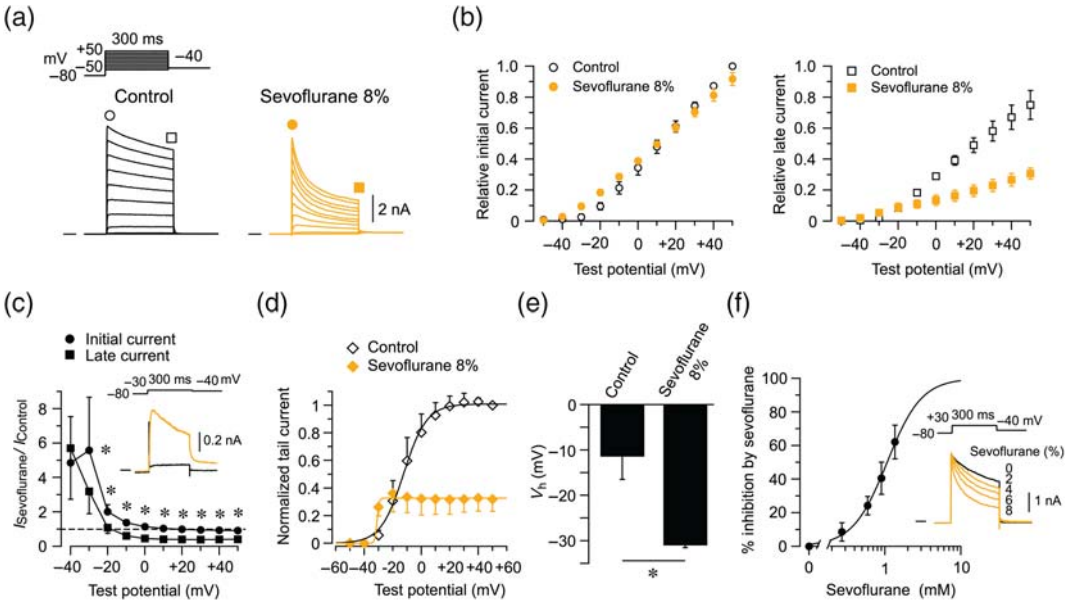

FIGURE 6 Modulatory effects of sevoflurane on $hK_v1.5$ current. (a) Superimposed traces of $hK_v1.5$ currents activated during 300-ms depolarizing steps to test potentials of −50 to +50 mV in 10 mV steps applied from a holding potential of −80 mV, before (left panel, Control) and 6 min after exposure to 8% sevoflurane (right panel). The voltage-clamp protocol is illustrated above the control traces of hKv1.5 current. (b) The current–voltage relationships for the initial (left panel) and late current levels (right panel) measured during depolarizing steps in control and in the presence of 8% sevoflurane. The amplitude of initial or late current at each test potential was normalized with reference to its initial current amplitude measured at +50 mV in control (n = 6). (c) The ratio of initial or late current amplitudes measured in the absence and presence of 8% sevoflurane, obtained by dividing the current amplitude in the presence of sevoflurane by that in its absence at each test potential ($I_{Sevoflurane}/I_{Control}$). The dashed line indicates $I_{Sevoflurane}/I_{Control}$ = 1. *P < 0.05 between the ratio of initial and late current amplitudes at each test potential. (d) The current–voltage relationships for the tail currents of hKv1.5 channel in the absence and presence of 8% sevoflurane. The smooth curves through the data points represent least-squares fittings of the Boltzmann equation to the data points, yielding V_h. (e) V_h for the voltage-dependent activation of $hK_v1.5$ current in control and in the presence of 8% sevoflurane. *P < 0.05, compared with control. n = 6 in each group. (f) Mean concentration–response relationships for the inhibition of $hK_v1.5$ current by sevoflurane. The data points (n = 6) represent the percent inhibition of late current, calculated as the reduction with respect to control value measured at the end of 300-ms depolarizing step to +30 mV. The smooth curve through the data points represents a least-squares fit of Hill equation, yielding an IC_{50} of 1.01 ± 0.14 mM, which corresponds to 6.9 ± 1.0% (n = 6). The concentration of sevoflurane is shown as millimolar order. Inset, superimposed traces of $hK_v1.5$ current recorded during 300-ms depolarizing step to +30 mV before and during exposure to increasing concentrations (2%, 4%, 6%, and 8%) of sevoflurane applied in a cumulative manner

3.7 | Docking simulation for interaction of desflurane or sevoflurane with $hK_v1.5$ channel

We further explored the structural information concerning the interaction of desflurane or sevoflurane with $hK_v1.5$ channels, using a computational docking simulation. Desflurane or sevoflurane can be docked into the multiple sites within the $hK_v1.5$ channel, including the inner cavity of the pore, S6-pore helix interface, extracellular face, S4-S5 linker, voltage-sensor domain, and S4-pore interface (Figures S1 and S2). The present electrophysiological experiments supported the view that desflurane and sevoflurane act as an open-channel blocker on $hK_v1.5$ channels by affecting several amino acids, including Thr480, Val505, and Ile508 (Figures 4 and 8). Because these amino acids are predicted to face toward the inner cavity of the pore (Eldstrom & Fedida, 2009), we primarily focused on the channel pore region in following docking simulations.

The docking simulation, limited to within the channel pore region, predicted that desflurane or sevoflurane was positioned near the base of the ion selectivity filter (Figure 9a,c, respectively) and that amino acids within a distance of 4.5 Å from desflurane or sevoflurane at this position were Thr479, Thr480, Val505, and Ile508 (Figure 9b,d, respectively). The binding free energies of desflurane and sevoflurane at this position were calculated to be −3.55 and −3.65 kcal mol^{-1}, respectively.

In silico alanine scanning mutagenesis was conducted for $hK_v1.5$ channel with docked desflurane or sevoflurane (Figure 10a,b, respectively), which revealed that the binding energy of desflurane or sevoflurane was decreased in T480A, V505A, and I508A mutant channels compared with WT channel (Figure 10c,d, respectively). However, the binding energy of desflurane or sevoflurane was unchanged or slightly increased in T479A mutant channel, respectively (Figure 10c,d, respectively). These results suggest that the specific

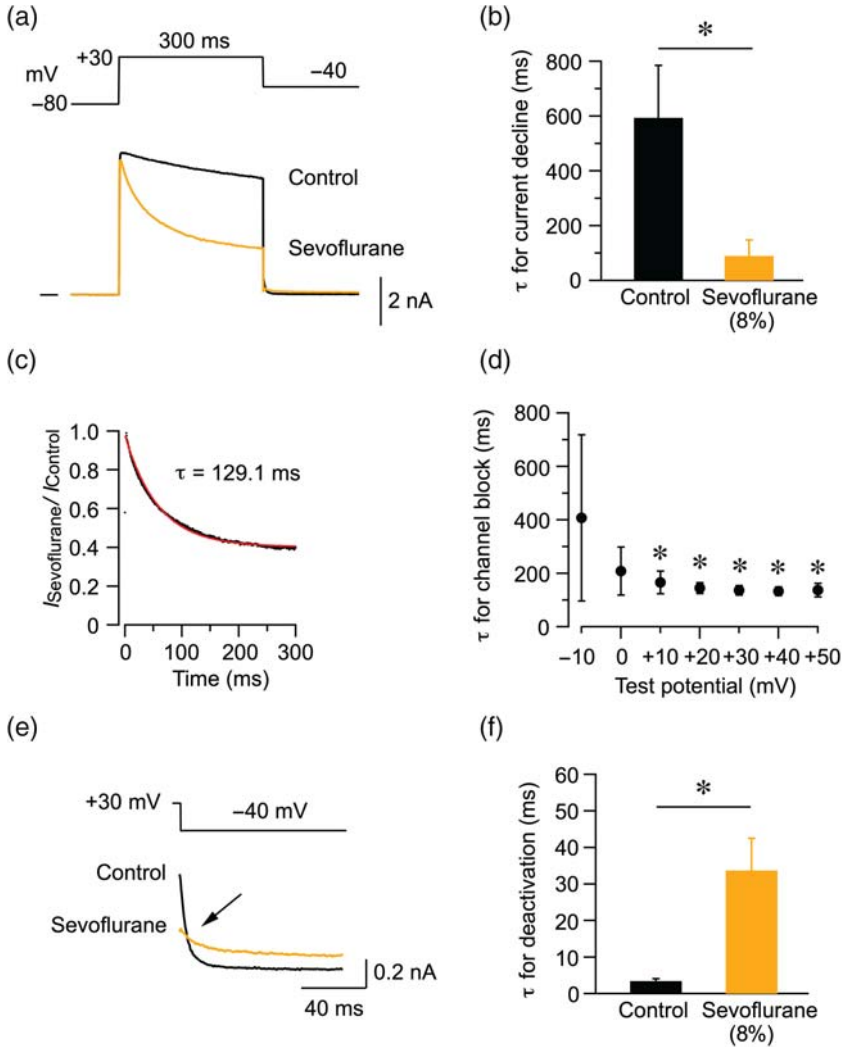

FIGURE 7 Open-channel blocking effect of sevoflurane on $hK_v1.5$ channels. (a) Superimposed $hK_v1.5$ currents recorded during 300-ms depolarizing step to +30 mV before and during exposure to 8% sevoflurane. (b) Time constant (τ) for the $hK_v1.5$ current decline during 300-ms depolarizing steps in the absence (Control) and presence of 8% sevoflurane, obtained by least-squares fitting of single exponential function. *P < 0.05 between control and 8% sevoflurane groups (n = 6). (c) The current ratio ($I_{Sevoflurane}/I_{Control}$) obtained by dividing $hK_v1.5$ current in the presence of 8% sevoflurane ($I_{Sevoflurane}$) by that in its absence ($I_{Control}$), shown in Figure 7a. The smooth curve through the data points (red) represents a least-squares fit of a single exponential function, yielding a time constant for channel block (τ). (d) Time constant (τ) for $hK_v1.5$ channel inhibition by sevoflurane at various test potentials (n = 6). *P < 0.05, compared with τ at −10 mV. (e) Superimposed tail currents elicited upon repolarization to −40 mV following depolarizing steps to +30 mV in the absence (Control) and presence of 8% sevoflurane. The arrow shows crossover of tail currents. (f) The time constant (τ) for the decay of tail currents in the absence and presence of 8% sevoflurane, obtained by the least-squares fit of the single exponential function. *P < 0.05 between control and 8% sevoflurane groups (n = 6)

amino acids Thr480, Val505, and Ile508 in $hK_v1.5$ channel are involved in the interaction with desflurane or sevoflurane.

3.8 | Mutational analysis of desflurane-induced positive modulation of $hK_v1.5$ channel

Desflurane has a positive modulatory effect on $hK_v1.5$ channels, which is prominent at mild depolarizations (Figure 1). We examined whether point mutations of amino acids within the pore region of $hK_v1.5$ channel affect the positive modulation by desflurane. Figure S3A shows the current ratio ($I_{Desflurane}/I_{Control}$) at the initial and late current levels at each test potential recorded from WT and eight selected mutant $hK_v1.5$ channels. When analysed at a test potential of −30 mV, where the positive modulatory effect of desflurane was most evident in WT channel, a similar positive modulatory action of desflurane was observed in T462C, H463C, T479A, T480A, R487V, A501V, I502A, and V516A mutant channels (Figure S3B,C). In contrast, this stimulatory action of desflurane was significantly reduced or even abolished in V505A, I508A, A509G, L510A, and V512A mutant channels. Thus, some point mutations within the S6 region, namely, V505A, I508A, A509G, L510A, and V512A, affected the stimulatory effect of desflurane on $hK_v1.5$ channels at weak depolarizations.

3.9 | Inhibitory effects of desflurane on hERG and hKCNQ1/hKCNE1 channels

We then compared the sensitivity to desflurane among three repolarizing K^+ currents in human heart, namely, $hK_v1.5$, hERG, and hKCNQ1/hKCNE1 currents, which underlie I_{Kur}, I_{Kr}, and I_{Ks}, respectively (Fedida et al., 1993; Keating & Sanguinetti, 2001). Figure S4A–D shows the effects of 18% desflurane on hERG and hKCNQ1/hKCNE1 currents. The inhibitory effect of 18% desflurane on $hK_v1.5$, hERG, and hKCNQ1/hKCNE1 channels was evaluated by measuring the amplitudes of tail currents fitted with the Boltzmann equation (Figures 1d and S4B,D). The inhibitory potency of desflurane was larger in the order of hKCNQ1/hKCNE1, $hK_v1.5$, and hERG channels, as judged from their IC_{50} values (Figure S4E), obtained from the concentration–response relationships for reduction of membrane currents (hKV1.5, Figure 3c; hERG and hKCNQ1/hKCNE1, data not shown). Desflurane shifted V_h in $hK_v1.5$ channels in a negative

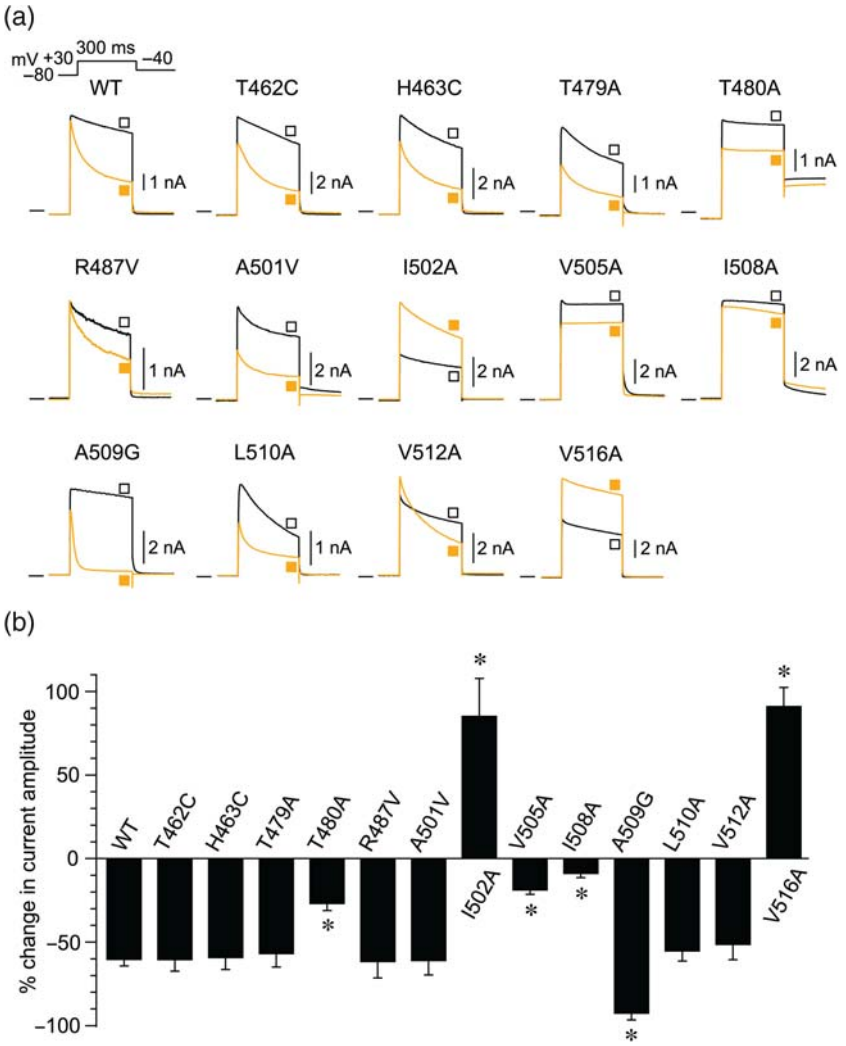

FIGURE 8 Effect of 8% sevoflurane on wild-type (WT) and mutant $hK_v1.5$ channel currents. (a) Superimposed current traces recorded from WT and 13 mutant $hK_v1.5$ channels (T462C, H463C, T479A, T480A, R487V, A501V, I502A, V505A, I508A, A509G, L510A, V512A, and V516A) during 300-ms depolarizing step to +30 mV in the absence (open square) and presence (filled square) of 8% sevoflurane. (b) The percent change in the late current amplitude at +30 mV caused by 8% sevoflurane in WT and 13 mutant hKv1.5 channel currents. *$P < 0.05$, compared with WT. $n = 6$ in each group

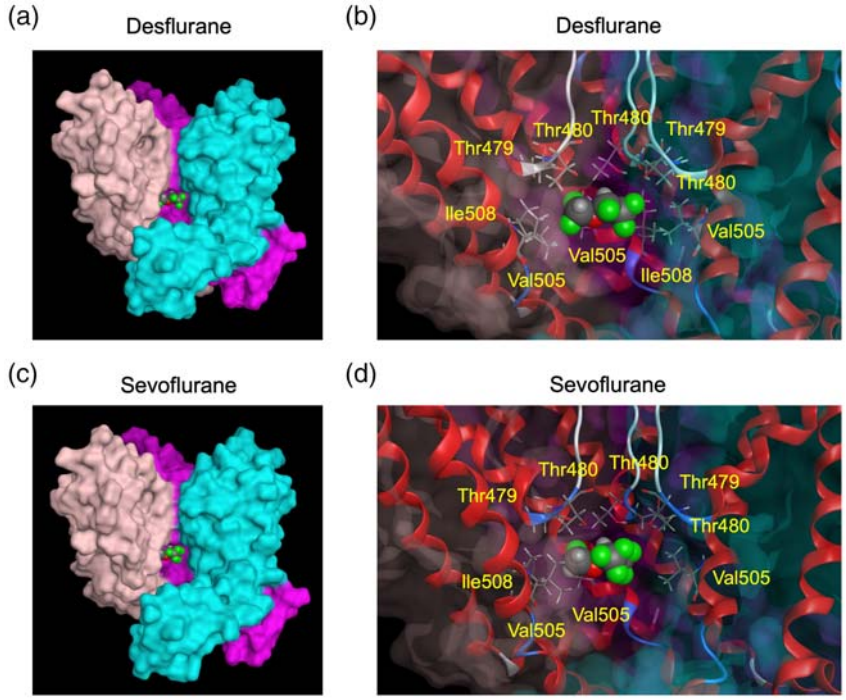

FIGURE 9 A simulated docking pose of desflurane or sevoflurane within the pore region of the open-state model of $hK_v1.5$ channel. (a and b) A side view (a) and expanded version (b) of the docked desflurane within the inner cavity of the $hK_v1.5$ channel pore. (c and d) A side view (c) and expanded version (d) of the docked sevoflurane within the inner cavity of $hK_v1.5$ channel pore. Desflurane or sevoflurane was located near the base of the ion selectivity filter with the lowest docking score in the docking simulation limited within the channel pore region. Only three pore domains are shown for clarity. Desflurane and sevoflurane are shown as a space-filled model, and the amino acids predicted to reside within 4.5 Å from anaesthetics (Thr479, Thr480, Val505, and Ile508) are shown in a stick format

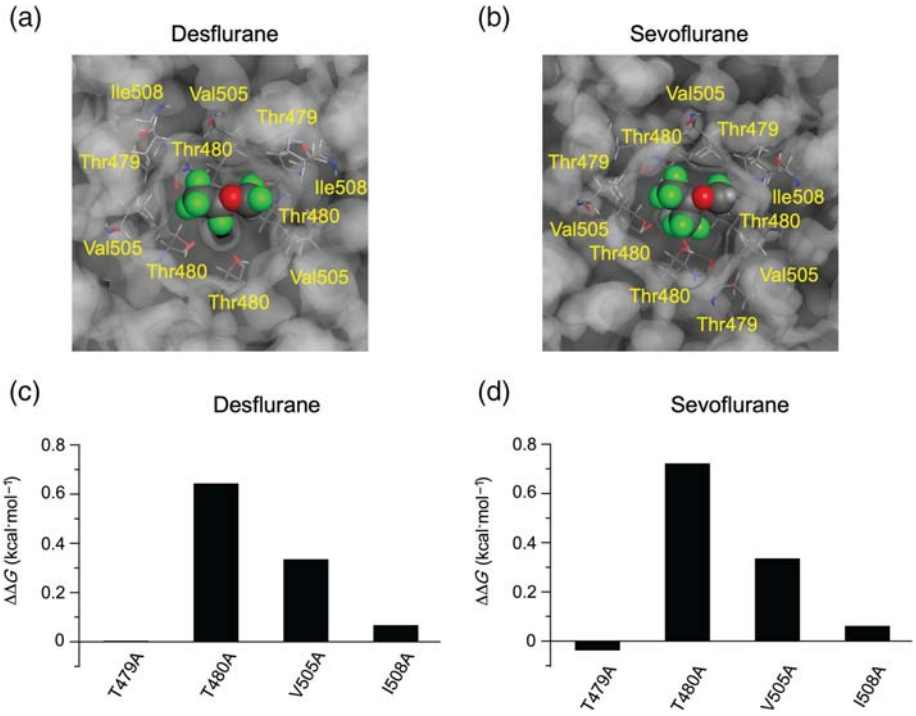

FIGURE 10 Changes in binding free energies by *in silico* alanine scanning mutagenesis in $hK_v1.5$ channel. (a and b) Pore domains of $hK_v1.5$ channel with docked desflurane (a) or sevoflurane (b) at the lowest docking score in the docking simulation limited within the channel pore region, as viewed from the intracellular side. Desflurane and sevoflurane are shown as a space-filled model, and the amino acids predicted to reside within 4.5 Å from ligand (Thr479, Thr480, Val505, and Ile508) are shown in a stick format. (c and d) Differences in the binding free energy ($\Delta\Delta G$) for desflurane (c) or sevoflurane (d), calculated before and after *in silico* alanine scanning mutagenesis of Thr479, Thr480, Val505, and Ile508 in $hK_v1.5$ channel

direction but did not significantly alter V_h in hERG and hKCNQ1/hKCNE1 channels (Figure S4F). Figure S4G illustrates a sequence alignment in the range between the selectivity filter and S6 in $hK_v1.5$, hERG, and hKCNQ1/hKCNE1 channels. The hKv1.5 channel has 23.3% homology with hERG and 41.9% homology with hKCNQ1 in these regions. This relatively low homology among these three K^+ channels may explain the substantial differences in the sensitivity to inhibition by desflurane (Figure S4E).

4 | DISCUSSION

A previous electrophysiological study using a heterologous expression system has examined the effects of sevoflurane on $K_v1.x$-family (*Shaker*-related) channels (**$K_v1.1$**, $K_v1.2$, **$K_v1.3$**, **$K_v1.4$**, and $K_v1.5$ channels) in detail and found that there are substantial differences in the sensitivity to sevoflurane among these $K_v1.x$ channel members (Lioudyno et al., 2013). For example, whereas sevoflurane potentiates $rK_v1.2$ current at all test potentials ranging from −50 to +40 mV, sevoflurane potentiates $hK_v1.5$ current at low depolarizing test potentials of ≤−10 mV but decreases it at higher voltages of ≥0 mV (Lioudyno et al., 2013). This voltage-dependent dual effect of sevoflurane on $hK_v1.5$ channels was confirmed in the present study (Figure 6). It is thus evident that the modulatory action of sevoflurane differs considerably between $K_v1.2$ and $K_v1.5$ channels.

The present experiments also found that desflurane has voltage-dependent positive and negative modulatory effects on $hK_v1.5$ current (Figure 1), which appears to be qualitatively similar to the effects of sevoflurane (Figure 6). The negative modulation of $hK_v1.5$ channels by desflurane and sevoflurane is characterized as follows: (i) $hK_v1.5$ current reduction was minimal at the onset of depolarization but gradually proceeded during the depolarizing steps of 300-ms duration (Figures 2a–c and 7a–c), (ii) the reduction of $hK_v1.5$ current became faster at more depolarized potentials (Figures 2d and 7d), where the open probability of the channel was elevated (Figures 1d and 6d), and (iii) the deactivation process was hampered (Figures 2e,f and 7e,f), possibly because the $hK_v1.5$ channel can only close after volatile anaesthetics are expelled from its binding sites within the channel pore (Decher et al., 2006). All these characteristics are consistent with desflurane or sevoflurane preferentially affecting the $hK_v1.5$ channel in its open-state to produce an inhibitory modulation (open-channel blockade).

It is generally accepted that open-channel blockers on ion channels, including $hK_v1.5$ channels, enter the inner vestibule of the channel pore during its open-state and interact with specific amino acids within the pore domain of channel. Several amino acids within $hK_v1.5$ channel, including Thr479, Thr480, Val505, Ile508, Val512, and Val516, have been suggested to face toward the inner cavity of the channel pore (Eldstrom & Fedida, 2009). These amino acids are regarded as putative binding sites for various open-channel blockers of $hK_v1.5$ channel, such as S0100176 (Decher et al., 2004), AVE0118 (Decher et al., 2006), vernakalant (Eldstrom et al., 2007), propofol (Kojima et al., 2018), and **verapamil** (Ding et al., 2019), by previous mutagenesis and docking simulation analyses. It should be noted that these previous docking simulations were conducted on a rigid receptor ($hK_v1.5$ channel) without being equilibrated and embedded in the lipid bilayer. The present site-directed mutagenesis also suggests that Thr480, Val505, and Ile508 are involved in mediating the open-channel blocking action of desflurane and sevoflurane on $hK_v1.5$ channels (Figures 4, 5, and 8).

Interestingly, the blocking effect of desflurane or sevoflurane on $hK_v1.5$ channels was potentiated in A509G mutant channel

(Figures 4, 5, and 8). Because the A509G mutation is accompanied by a retraction in side chain mass at position 509 (Eldstrom & Fedida, 2009), it seems likely that the orientation of the side chain of neighbouring amino acids such as Val505 and Ile508 is altered. In that case, anaesthetics can more readily interact with its putative target amino acids, such as Val505 and Ile508, resulting in potentiation of the blocking potency of anaesthetics. Thus, Ala509 appears to play a certain role in determining the degree to which $hK_v1.5$ channels are blocked by desflurane and sevoflurane.

We also found that desflurane and sevoflurane exclusively increase amplitudes of I502A and V516A mutant channels (Figures 4 and 8). A previous study showed that substitution of alanine for proline at position 410 (P410A) in the S6 segment of the *Drosophila* voltage-gated potassium channel Shaw2 converts the modulation by 1-alkanols from inhibition to potentiation (Harris et al., 2003). Although the precise mechanism has yet to be fully elucidated, it seems likely that substitution of specific amino acids within S6 segment of voltage-gated potassium channel could cause a drastic alteration in response to general anaesthetics. It is thus assumed that the presence of isoleucine and valine at positions 502 and 516, respectively, is required to confer the proper blocking effect of desflurane and sevoflurane on $hK_v1.5$ channels.

Because site-directed mutagenesis can be accompanied by allosteric conformational changes, we used the other experimental approach computational docking simulation to obtain structural information concerning the interaction of desflurane or sevoflurane with $hK_v1.5$ channel. The present docking simulation showed that desflurane and sevoflurane can reside within various regions of $hK_v1.5$ channel, including the inner cavity of channel pore (Figures S1 and S2). When the docking site is limited within the pore region, desflurane and sevoflurane can be located adjacent to Thr479, Thr480, Val505, and Ile508 (Figure 9). *In silico* alanine scanning demonstrated that binding free energy of desflurane or sevoflurane was decreased by mutations at Thr480, Val505, and Ile508 (Figure 10), which is qualitatively consistent with the results obtained by site-directed mutagenesis and patch-clamp experiments (Figures 4 and 8). Thus, whereas desflurane and sevoflurane can bind to multiple sites within $hK_v1.5$ channels, these three amino acids (Thr480, Val505, and Ile508) within the channel pore appear to be important for producing an open-channel blocking action of desflurane and sevoflurane.

It is interesting to note that the amino acid sequence in pore region, associated with binding sites for open-channel blockers, considerably differs among the different classes of voltage-gated potassium channels, such as $hK_v1.5$, hERG, and hKCNQ1/hKCNE1 channels (Decher et al., 2004; Eldstrom et al., 2007). For example, isoleucine at position 508 in $hK_v1.5$ channels corresponds to tyrosine at position 652 in hERG channels or phenylalanine at position 340 in hKCNQ1 channels (Figure S4G). A previous study has shown that the replacement of isoleucine at position 508 with tyrosine in $hK_v1.5$ channel decreases the inhibitory potency of vernakalant to near the level for hERG channel (Eldstrom et al., 2007). The present experiments have also revealed that there are considerable differences in inhibitory potency of desflurane among $hK_v1.5$, hERG, and hKCNQ1/hKCNE1 channels (Figure S4). Although the possible molecular basis for the inhibitory action of desflurane on these voltage-gated K^+ channels has yet to be fully elucidated, considerable differences in amino acid sequences in putative binding sites may be related, at least in part, to the differences in the inhibitory potency of desflurane.

There are several limitations in our study. While mutagenesis experiments are associated with allosteric effects, computational docking simulations cannot completely reproduce the physiological cellular milieu involved in drug–channel interaction. Furthermore, although previous workers have adopted an innovative approach of ionic flux simulations under applied transmembrane voltages to investigate channel-anaesthetic interaction (Stock et al., 2018), our simulation study did not reproduce K^+ efflux through the fully flexible channel protein embedded in cell membranes. Because our site-directed mutagenesis and docking simulation experiments were conducted by focusing on the channel pore region, our studies do not necessarily rule out other molecular mechanisms underlying the open-channel blocking action of desflurane and sevoflurane on $hK_v1.5$ channels. For example, these anaesthetics can interact with other regions of channel proteins (Figures S1 and S2) or even the lipid bilayer of the cell membrane (Sonner & Cantor, 2013) to produce modulatory actions on $hK_v1.5$ channels. It is interesting to note that volatile anaesthetics exert an open-channel blocking action on $hK_v1.5$ channels but not on $K_v1.2$ channels (Lioudyno et al., 2013), although these two channels exhibit approximately 90% homology in amino acid sequences in the pore region (Eldstrom et al., 2007). Further studies are required to extensively examine the possible involvement of other sites of channel proteins in mediating the open-channel blocking action of the drugs.

The $K_v1.5$ channel has been shown to regulate the membrane potential and thereby contractility in pulmonary artery smooth muscle cells (Cogolludo et al., 2006; Hayabuchi, 2017). It is therefore expected that desflurane- or sevoflurane-induced modulation of $hK_v1.5$ channels can affect the regulation of pulmonary artery resistance in a complicated way (Kerbaul et al., 2004; Lennon & Murray, 1996). Because $hK_v1.5$ channels are also responsible for action potential repolarization in human atrium (Wettwer et al., 2004), desflurane or sevoflurane can influence the refractoriness in the human atrium.

In conclusion, the present study found that desflurane and sevoflurane have stimulatory and inhibitory effects on the human $K_v1.5$ channel and that their inhibitory effects arise from an open-channel blocking action by interacting with the channel pore. These findings provide information about new target sites for the modulation of $hK_v1.5$ channels by volatile anaesthetics and mechanisms underlying electrophysiological alteration of cardiac or vascular functions by volatile anaesthetics in the clinical setting.

ACKNOWLEDGEMENTS

The authors are grateful to Professor David Fedida (Department of Physiology, University of British Columbia, Vancouver, Canada), Professor Michael Sanguinetti (University of Utah, Salt Lake City, UT, USA), and Professor Jacques Barhanin (Institut de Pharmacologie

Moléculaire et Cellulaire, CNRS, Valbonne, France) for kindly providing the full-length cDNA (cDNA) encoding the human wild-type $K_v1.5$ channel, human ether-a-go-go-related gene (hERG) channel, and human KCNQ1 channel, respectively. The authors also thank Dr. Tomoyoshi Seto (Department of Anesthesiology, Shiga University of Medical Science, Otsu, Shiga, Japan) for valuable comments on docking simulation experiments. This study was supported by JSPS (The Japan Society for the Promotion of Science, Tokyo, Japan) KAKENHI Grants 18K16445 (to Y.F.), 17K11050 (to A.K.), and 17K08536 (to H.M.).

AUTHOR CONTRIBUTIONS

Y.F., A.K., and H.M. designed the experiments. Y.F. conducted the experiments. Y.F., A.K., and H.M. analysed the data. Y.F., A.K., X.M., W.-G.D., H.K., and H.M. participated in the data interpretation. Y.F., A.K., and H.M. wrote the manuscript. Y.F., A.K., X.M., W.-G.D., H.K., and H.M. approved the final manuscript.

CONFLICT OF INTEREST

The authors declare no conflicts of interest.

DECLARATION OF TRANSPARENCY AND SCIENTIFIC RIGOUR

This Declaration acknowledges that this paper adheres to the principles for transparent reporting and scientific rigour of preclinical research as stated in the *BJP* guidelines for Design & Analysis, and as recommended by funding agencies, publishers and other organisations engaged with supporting research.

ORCID

Akiko Kojima https://orcid.org/0000-0002-9649-5495
Hiroshi Matsuura https://orcid.org/0000-0003-1998-0996

REFERENCES

Alexander, S. P. H., Mathie, A., Peters, J. A., Veale, E. L., Striessnig, J., Kelly, E., … Sharman, J. L. (2019). The concise guide to pharmacology 2019/20: Ion channels. *British Journal of Pharmacology*, *176*(Suppl 1), S142–S228.

Aranake, A., Mashour, G. A., & Avidan, M. S. (2013). Minimum alveolar concentration: Ongoing relevance and clinical utility. *Anaesthesia*, *68*, 512–522. https://doi.org/10.1111/anae.12168

Bai, J. Y., Ding, W. G., Kojima, A., Seto, T., & Matsuura, H. (2015). Putative binding sites for arachidonic acid on the human cardiac Kv 1.5 channel. *British Journal of Pharmacology*, *172*, 5281–5292. https://doi.org/10.1111/bph.13314

Barber, A. F., Liang, Q., & Covarrubias, M. (2012). Novel activation of voltage-gated K^+ channels by sevoflurane. *The Journal of Biological Chemistry*, *287*, 40425–40432. https://doi.org/10.1074/jbc.M112.405787

Chutiwitoonchai, N., Hiyoshi, M., Mwimanzi, P., Ueno, T., Adachi, A., Ode, H., … Suzu, S. (2011). The identification of a small molecule compound that reduces HIV-1 Nef-mediated viral infectivity enhancement. *PLoS ONE*, *6*, e27696. https://doi.org/10.1371/journal.pone.0027696

Cogolludo, A., Moreno, L., Lodi, F., Frazziano, G., Cobeno, L., Tamargo, J., & Perez-Vizcaino, F. (2006). Serotonin inhibits voltage-gated K^+ currents in pulmonary artery smooth muscle cells: Role of 5-HT2A receptors, caveolin-1, and Kv1.5 channel internalization. *Circulation Research*, *98*, 931–938. https://doi.org/10.1161/01.RES.0000216858.04599.e1

Corbeil, C. R., Williams, C. I., & Labute, P. (2012). Variability in docking success rates due to dataset preparation. *Journal of Computer-Aided Molecular Design*, *26*, 775–786. https://doi.org/10.1007/s10822-012-9570-1

Covarrubias, M., Barber, A. F., Carnevale, V., Treptow, W., & Eckenhoff, R. G. (2015). Mechanistic insights into the modulation of voltage-gated ion channels by inhalational anesthetics. *Biophysical Journal*, *109*, 2003–2011. https://doi.org/10.1016/j.bpj.2015.09.032

Curtis, M. J., Alexander, S., Cirino, G., Docherty, J. R., George, C. H., Giembycz, M. A., … Ahluwalia, A. (2018). Experimental design and analysis and their reporting II: Updated and simplified guidance for authors and peer reviewers. *British Journal of Pharmacology*, *175*, 987–993. https://doi.org/10.1111/bph.14153

Decher, N., Kumar, P., Gonzalez, T., Pirard, B., & Sanguinetti, M. C. (2006). Binding site of a novel Kv1.5 blocker: A "foot in the door" against atrial fibrillation. *Molecular Pharmacology*, *70*, 1204–1211. https://doi.org/10.1124/mol.106.026203

Decher, N., Pirard, B., Bundis, F., Peukert, S., Baringhaus, K. H., Busch, A. E., … Sanguinetti, M. C. (2004). Molecular basis for Kv1.5 channel block: Conservation of drug binding sites among voltage-gated K^+ channels. *The Journal of Biological Chemistry*, *279*, 394–400. https://doi.org/10.1074/jbc.M307411200

Ding, W. G., Tano, A., Mi, X., Kojima, A., Seto, T., & Matsuura, H. (2019). Identification of verapamil binding sites within human Kv1.5 channel using mutagenesis and docking simulation. *Cellular Physiology and Biochemistry*, *52*, 302–314. https://doi.org/10.33594/000000022

Eduljee, C., Claydon, T. W., Viswanathan, V., Fedida, D., & Kehl, S. J. (2007). SCAM analysis reveals a discrete region of the pore turret that modulates slow inactivation in Kv1.5. *American Journal of Physiology. Cell Physiology*, *292*, C1041–C1052. https://doi.org/10.1152/ajpcell.00274.2006

Eldstrom, J., & Fedida, D. (2009). Modeling of high-affinity binding of the novel atrial anti-arrhythmic agent, vernakalant, to Kv1.5 channels. *Journal of Molecular Graphics & Modelling*, *28*, 226–235. https://doi.org/10.1016/j.jmgm.2009.07.005

Eldstrom, J., Wang, Z., Xu, H., Pourrier, M., Ezrin, A., Gibson, K., & Fedida, D. (2007). The molecular basis of high-affinity binding of the antiarrhythmic compound vernakalant (RSD1235) to Kv1.5 channels. *Molecular Pharmacology*, *72*, 1522–1534. https://doi.org/10.1124/mol.107.039388

Fedida, D., Wible, B., Wang, Z., Fermini, B., Faust, F., Nattel, S., & Brown, A. M. (1993). Identity of a novel delayed rectifier current from human heart with a cloned K^+ channel current. *Circulation Research*, *73*, 210–216. https://doi.org/10.1161/01.RES.73.1.210

Franks, N. P. (2006). Molecular targets underlying general anaesthesia. *British Journal of Pharmacology*, *147*(Suppl 1), S72–S81.

Franks, N. P. (2008). General anaesthesia: From molecular targets to neuronal pathways of sleep and arousal. *Nature Reviews. Neuroscience*, *9*, 370–386. https://doi.org/10.1038/nrn2372

Friederich, P., Benzenberg, D., Trellakis, S., & Urban, B. W. (2001). Interaction of volatile anesthetics with human Kv channels in relation to clinical concentrations. *Anesthesiology*, *95*, 954–958. https://doi.org/10.1097/00000542-200110000-00026

Goto, J., Kataoka, R., Muta, H., & Hirayama, N. (2008). ASEDock-docking based on alpha spheres and excluded volumes. *Journal of Chemical Information and Modeling*, *48*, 583–590. https://doi.org/10.1021/ci700352q

Hamill, O. P., Marty, A., Neher, E., Sakmann, B., & Sigworth, F. J. (1981). Improved patch-clamp techniques for high-resolution current recording from cells and cell-free membrane patches. *Pflügers Archiv*, *391*, 85–100. https://doi.org/10.1007/BF00656997

Harding, S. D., Sharman, J. L., Faccenda, E., Southan, C., Pawson, A. J., Ireland, S., … NC-IUPHAR. (2018). The IUPHAR/BPS guide to pharmacology in 2018: Updates and expansion to encompass the new guide to immunopharmacology. *Nucleic Acids Research*, *46*, D1091–D1106. https://doi.org/10.1093/nar/gkx1121

Harris, T., Graber, A. R., & Covarrubias, M. (2003). Allosteric modulation of a neuronal K^+ channel by 1-alkanols is linked to a key residue in the activation gate. *American Journal of Physiology. Cell Physiology*, *285*, C788–C796. https://doi.org/10.1152/ajpcell.00113.2003

Hayabuchi, Y. (2017). The action of smooth muscle cell potassium channels in the pathology of pulmonary arterial hypertension. *Pediatric Cardiology*, *38*, 1–14. https://doi.org/10.1007/s00246-016-1491-7

Hemmings, H. C., Akabas, M. H., Goldstein, P. A., Trudell, J. R., Orser, B. A., & Harrison, N. L. (2005). Emerging molecular mechanisms of general anesthetic action. *Trends in Pharmacological Sciences*, *26*, 503–510. https://doi.org/10.1016/j.tips.2005.08.006

Hiasa, M., Isoda, Y., Kishimoto, Y., Saitoh, K., Kimura, Y., Kanai, M., … Kuzuhara, T. (2013). Inhibition of MAO-A and stimulation of behavioural activities in mice by the inactive prodrug form of the anti-influenza agent oseltamivir. *British Journal of Pharmacology*, *169*, 115–129. https://doi.org/10.1111/bph.12102

Hudson, A. E., Herold, K. F., & Hemmings, H. C. Jr. (2018). *Pharmacology and physiology for anesthesia* (2nd ed.). Philadelphia, PA, USA: Elsevier Inc.

Kang, J., Reynolds, W. P., Chen, X. L., Ji, J., Wang, H., & Rampe, D. E. (2006). Mechanisms underlying the QT interval-prolonging effects of sevoflurane and its interactions with other QT-prolonging drugs. *Anesthesiology*, *104*, 1015–1022. https://doi.org/10.1097/00000542-200605000-00018

Keating, M. T., & Sanguinetti, M. C. (2001). Molecular and cellular mechanisms of cardiac arrhythmias. *Cell*, *104*, 569–580. https://doi.org/10.1016/S0092-8674(01)00243-4

Kerbaul, F., Rondelet, B., Motte, S., Fesler, P., Hubloue, I., Ewalenko, P., … Brimioulle, S. (2004). Isoflurane and desflurane impair right ventricular-pulmonary arterial coupling in dogs. *Anesthesiology*, *101*, 1357–1362. https://doi.org/10.1097/00000542-200412000-00016

Kojima, A., Fukushima, Y., Ito, Y., Ding, W. G., Ueda, R., Seto, T., … Matsuura, H. (2018). Interactions of propofol with human voltage-gated Kv1.5 channel determined by docking simulation and mutagenesis analyses. *Journal of Cardiovascular Pharmacology*, *71*, 10–18. https://doi.org/10.1097/FJC.0000000000000538

Kojima, A., Ito, Y., Ding, W. G., Kitagawa, H., & Matsuura, H. (2015). Interaction of propofol with voltage-gated human Kv1.5 channel through specific amino acids within the pore region. *European Journal of Pharmacology*, *764*, 622–632. https://doi.org/10.1016/j.ejphar.2015.08.007

Kojima, A., Ito, Y., Kitagawa, H., Matsuura, H., & Nosaka, S. (2014). Direct negative chronotropic action of desflurane on sinoatrial node pacemaker activity in the guinea pig heart. *Anesthesiology*, *120*, 1400–1413. https://doi.org/10.1097/ALN.0000000000000165

Labute, P. (2008). The generalized Born/volume integral implicit solvent model: Estimation of the free energy of hydration using London dispersion instead of atomic surface area. *Journal of Computational Chemistry*, *29*, 1693–1698. https://doi.org/10.1002/jcc.20933

Labute, P. (2009). Protonate3D: Assignment of ionization states and hydrogen coordinates to macromolecular structures. *Proteins*, *75*, 187–205. https://doi.org/10.1002/prot.22234

Lennon, P. F., & Murray, P. A. (1996). Attenuated hypoxic pulmonary vasoconstriction during isoflurane anesthesia is abolished by cyclooxygenase inhibition in chronically instrumented dogs. *Anesthesiology*, *84*, 404–414. https://doi.org/10.1097/00000542-199602000-00020

Li, Y., Xu, J., Xu, Y., Zhao, X. Y., Liu, Y., Wang, J., … Zhang, Z. (2018). Regulatory effect of general anesthetics on activity of potassium channels. *Neuroscience Bulletin*, *34*, 887–900. https://doi.org/10.1007/s12264-018-0239-1

Lioudyno, M. I., Birch, A. M., Tanaka, B. S., Sokolov, Y., Goldin, A. L., Chandy, K. G., … Alkire, M. T. (2013). Shaker-related potassium channels in the central medial nucleus of the thalamus are important molecular targets for arousal suppression by volatile general anesthetics. *The Journal of Neuroscience*, *33*, 16310–16322. https://doi.org/10.1523/JNEUROSCI.0344-13.2013

Liu, L. T., Willenbring, D., Xu, Y., & Tang, P. (2009). General anesthetic binding to neuronal α4β2 nicotinic acetylcholine receptor and its effects on global dynamics. *The Journal of Physical Chemistry. B*, *113*, 12581–12589. https://doi.org/10.1021/jp9039513

Liu, X., Peng, L., Zhou, Y., Zhang, Y., & Zhang, J. Z. H. (2018). Computational alanine scanning with interaction entropy for protein-ligand binding free energies. *Journal of Chemical Theory and Computation*, *14*, 1772–1780. https://doi.org/10.1021/acs.jctc.7b01295

Long, S. B., Campbell, E. B., & Mackinnon, R. (2005). Crystal structure of a mammalian voltage-dependent Shaker family K^+ channel. *Science*, *309*, 897–903. https://doi.org/10.1126/science.1116269

Mihic, S. J., Ye, Q., Wick, M. J., Koltchine, V. V., Krasowski, M. D., Finn, S. E., … Harrison, N. L. (1997). Sites of alcohol and volatile anaesthetic action on $GABA_A$ and glycine receptors. *Nature*, *389*, 385–389. https://doi.org/10.1038/38738

Mori, M., Matsuki, K., Maekawa, T., Tanaka, M., Sriwanthana, B., Yokoyama, M., & Ariyoshi, K. (2012). Development of a novel in silico docking simulation model for the fine HIV-1 cytotoxic T lymphocyte epitope mapping. *PLoS ONE*, *7*, e41703. https://doi.org/10.1371/journal.pone.0041703

Nishikawa, K., & Harrison, N. L. (2003). The actions of sevoflurane and desflurane on the γ-aminobutyric acid receptor type A: Effects of TM2 mutations in the α and β subunits. *Anesthesiology*, *99*, 678–684. https://doi.org/10.1097/00000542-200309000-00024

Nishio, Y., Makiyama, T., Itoh, H., Sakaguchi, T., Ohno, S., Gong, Y. Z., … Horie, M. (2009). D85N, a KCNE1 polymorphism, is a disease-causing gene variant in long QT syndrome. *Journal of the American College of Cardiology*, *54*, 812–819. https://doi.org/10.1016/j.jacc.2009.06.005

Postea, O., & Biel, M. (2011). Exploring HCN channels as novel drug targets. *Nature Reviews. Drug Discovery*, *10*, 903–914. https://doi.org/10.1038/nrd3576

Rudolph, U., & Antkowiak, B. (2004). Molecular and neuronal substrates for general anaesthetics. *Nature Reviews. Neuroscience*, *5*, 709–720. https://doi.org/10.1038/nrn1496

Saponara, S., Durante, M., Spiga, O., Mugnai, P., Sgaragli, G., Huong, T. T., … Fusi, F. (2016). Functional, electrophysiological and molecular docking analysis of the modulation of $Ca_v1.2$ channels in rat vascular myocytes by murrayafoline A. *British Journal of Pharmacology*, *173*, 292–304. https://doi.org/10.1111/bph.13369

Siegwart, R., Krähenbühl, K., Lambert, S., & Rudolph, U. (2003). Mutational analysis of molecular requirements for the actions of general anaesthetics at the γ-aminobutyric $acid_A$ receptor subtype, α1β2γ2. *BMC Pharmacology*, *3*, 13. https://doi.org/10.1186/1471-2210-3-13

Sonner, J. M., & Cantor, R. S. (2013). Molecular mechanisms of drug action: An emerging view. *Annual Review of Biophysics*, *42*, 143–167. https://doi.org/10.1146/annurev-biophys-083012-130341

Stock, L., Hosoume, J., Cirqueira, L., & Treptow, W. (2018). Binding of the general anesthetic sevoflurane to ion channels. *PLoS Computational Biology*, *14*, e1006605. https://doi.org/10.1371/journal.pcbi.1006605

Stock, L., Hosoume, J., & Treptow, W. (2017). Concentration-dependent binding of small ligands to multiple saturable sites in membrane proteins. *Scientific Reports*, *7*, 5734. https://doi.org/10.1038/s41598-017-05896-8

Trimmer, J. S. (2015). Subcellular localization of K^+ channels in mammalian brain neurons: Remarkable precision in the midst of extraordinary complexity. *Neuron*, *85*, 238–256. https://doi.org/10.1016/j.neuron.2014.12.042

Wettwer, E., Hala, O., Christ, T., Heubach, J. F., Dobrev, D., Knaut, M., … Ravens, U. (2004). Role of I_{Kur} in controlling action potential shape and

contractility in the human atrium: Influence of chronic atrial fibrillation. *Circulation*, *110*, 2299–2306. https://doi.org/10.1161/01.CIR.0000145155.60288.71

Woll, K. A., Peng, W., Liang, Q., Zhi, L., Jacobs, J. A., Maciunas, L., … Eckenhoff, R. G. (2017). Photoaffinity ligand for the inhalational anesthetic sevoflurane allows mechanistic insight into potassium channel modulation. *ACS Chemical Biology*, *12*, 1353–1362. https://doi.org/10.1021/acschembio.7b00222

Woll, K. A., Zhou, X., Bhanu, N. V., Garcia, B. A., Covarrubias, M., Miller, K. W., & Eckenhoff, R. G. (2018). Identification of binding sites contributing to volatile anesthetic effects on GABA type A receptors. *The FASEB Journal*, *32*, 4172–4189. https://doi.org/10.1096/fj.201701347R

Yellen, G. (2002). The voltage-gated potassium channels and their relatives. *Nature*, *419*, 35–42. https://doi.org/10.1038/nature00978

SUPPORTING INFORMATION

Additional supporting information may be found online in the Supporting Information section at the end of this article.

How to cite this article: Fukushima Y, Kojima A, Mi X, Ding W-G, Kitagawa H, Matsuura H. Open-channel blocking action of volatile anaesthetics desflurane and sevoflurane on human voltage-gated $K_v1.5$ channel. *Br J Pharmacol*. 2020; 177:3811–3827. https://doi.org/10.1111/bph.15105